

A Theoretical Method for an Accurate Elucidation of Energy Transfer Pathways in Europium(III) Complexes with Dipyridophenazine (dppz) Ligand. One more step in the Study of Molecular Antenna Effect.

María J. Beltrán-Leiva^a, Plinio Cantero-López^a, César Zúñiga^b, Ana Bulhões-Figueira^c,

Dayán Páez-Hernández^{a,b*}, Ramiro Arratia-Pérez^{a,b*}

dayan.paez@unab.cl, rarratia@unab.cl

^a Relativistic Molecular Physics (ReMoPh) Group, Ph.D. Program in Molecular Physical Chemistry, Universidad Andrés Bello, Av. República 275, Santiago 8370146, Chile. Tel/Fax: +56-2-2770-3352

^b Centro de Nanociencias Aplicadas, Facultad de Ciencias Exactas, Universidad Andrés Bello

^c Centro Universitário Estácio de Ribeirão Preto, Rua Abrahão Issa Halach, 980 - Ribeirânia, Ribeirão Preto - SP, 14096-160, Brazil.

Supporting Information

Contents

1. Structural Parameters	S3
Table S1.1. Bond lengths for [Eu(NO ₃) ₃ (dppz)] and [Eu(NO ₃) ₃ (H ₂ O) ₂ (dppz)] complexes.	S4
Table S1.2. Bond lengths for [Eu(NO ₃) ₃ (dppz-CN)] and [Eu(NO ₃) ₃ (H ₂ O) ₂ (dppz-CN)] complexes.	S5
Table S1.3. Bond lengths for [Eu(NO ₃) ₃ (dppz-NO ₂)] and [Eu(NO ₃) ₃ (H ₂ O) ₂ (dppz-NO ₂)] complexes.	S6
2. TD-DFT Calculations.....	S7
Table S2.1. Most relevant electronic transitions for dppz ligand.....	S7
Table S2.2. Molecular Orbitals involved in the electronic transitions for dppz ligand.....	S8
Table S2.3. Most important electronic transitions for dppz ligand with dichloromethane.	S10
Table S2.4. Molecular Orbitals involved in the electronic transitions for dppz ligand with dichloromethane.	S11

Table S2.5. Most important electronic transitions for dppz - CN ligand.....	S12
Table S2.6. Molecular Orbitals involved in the electronic transitions for dppz -CN ligand.	S13
Table S2.7. Most important electronic transitions for dppz - CN ligand with dichloromethane.	S15
Table S2.8. Molecular Orbitals involved in the electronic transitions for dppz-CN ligand with dichloromethane.....	S16
Table S2.9. Most important electronic transitions for dppz - NO ₂ ligand.	S17
Table S2.10. Molecular Orbitals involved in the electronic transitions for dppz- NO ₂ ligand.	S18
Table S2.11. Most important electronic transitions for dppz - NO ₂ ligand with dichloromethane.	S19
Table S2.12. Molecular Orbitals involved in the electronic transitions for dppz - NO ₂ with dichloromethane.	S20
3. Spin orbit energies for the low-lying states in the europium fragment.....	S21
Table S3. SO-CASPT2 energies for the Eu ^{III} fragments.....	S21
4. Experimental Section.....	S23
Figure S1. Top: experimental X-ray diffraction diagrams of the powders obtained with [Eu(NO ₃) ₃ (dppz-CN)].....	S25
Figure S2. Top: experimental X-ray diffraction diagrams of the powders obtained with [Eu(NO ₃) ₃ (dppz-NO ₂)]	S25
Figure S3. Proton and carbon numbering for the NMR signals of the dppz-CN ligand..	S26
Figure S4. Proton and carbon numbering for the NMR signals of the dppz-NO ₂ ligand	S27
Figure S5. ¹ H NMR spectrum of the dppz-CN ligand.....	S28
Figure S6. ¹ H NMR spectrum of the dppz-NO ₂ ligand.	S28
Figure S7. Decaying of the luminescence of the emitting ⁵ D ₀ Eu ^{III} state of the [Eu(NO ₃) ₃ (dppz-CN)].	S29
Figure S8. Decaying of the luminescence of the emitting ⁵ D ₀ Eu ^{III} state of the [Eu(NO ₃) ₃ (dppz-NO ₂)]......	S29
Figure S9. Film of complex [Eu(NO ₃) ₃ (dppz-NO ₂)] deposited in a round bottom flask, illuminated by a black light (ultraviolet light) lamp	S30

1. Structural Parameters

All structures were optimized employing the ADF package. Scalar relativistic effects were incorporated by means of the ZORA approximation. The BP86 functional was used with the TZ2P basis set. In all cases, frequency analysis were performed after the geometry optimization, where we obtained only positive frequencies indicating that the geometries obtained are in a true minimum. As can be observed, no significant conformational changes were produced between the ground and excited geometries. This is not surprising because all compounds have localized absorption and emission bands. Therefore, if an optimization of the excited and ground states were performed on both, ligands and lanthanide fragments, more pronounced changes on geometries could be noted.

Below, detailed geometrical parameters are presented for all complexes.

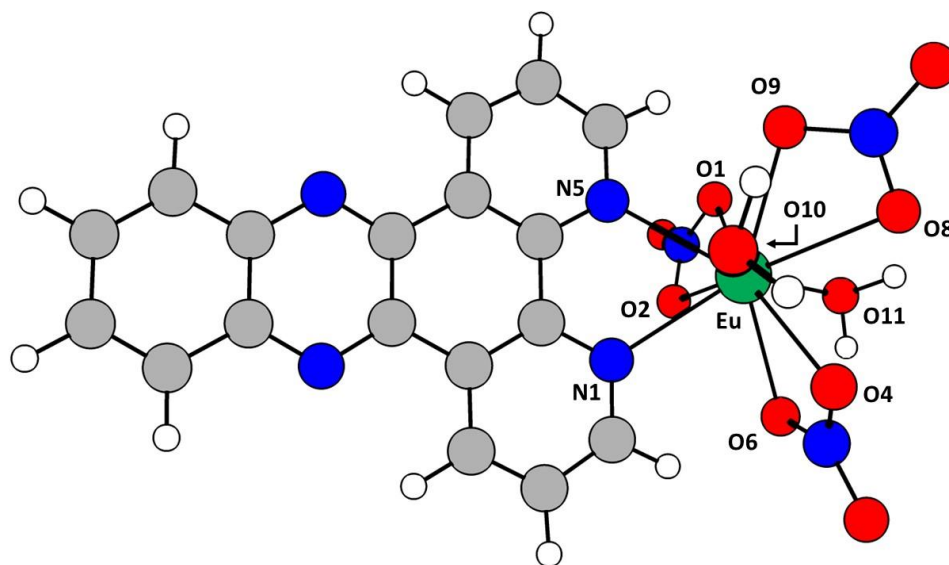
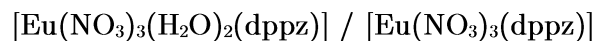


Table S1.1. Bond lengths for $[\text{Eu}(\text{NO}_3)_3(\text{dppz})]$ and $[\text{Eu}(\text{NO}_3)_3(\text{H}_2\text{O})_2(\text{dppz})]$ complexes. All distances are given in Å.

	$[\text{Eu}(\text{NO}_3)_3(\text{H}_2\text{O})_2(\text{dppz})]$		$[\text{Eu}(\text{NO}_3)_3(\text{dppz})]$	
	Ground	Excited	Ground	Excited
Eu-N1	2.697	2.687	2.627	2.616
Eu-N5	2.649	2.653	2.645	2.651
Eu-O1	2.456	2.462	2.466	2.473
Eu-O2	2.468	2.474	2.483	2.489
Eu-O4	2.511	2.503	2.464	2.452
Eu-O6	2.592	2.574	2.481	2.457
Eu-O8	2.538	2.559	2.485	2.502
Eu-O9	2.541	2.519	2.470	2.434
Eu-O10 _(h2o)	2.617	2.569	-	-
Eu-O11 _(h2o)	2.604	2.598	-	-

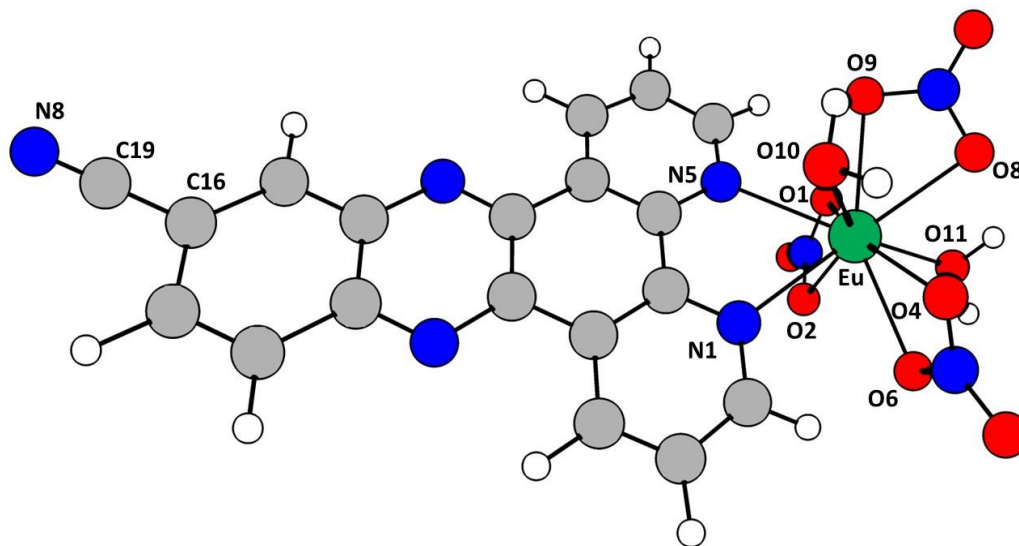
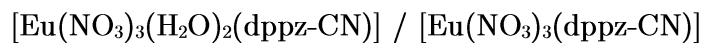


Table S1.2. Bond lengths for $[\text{Eu}(\text{NO}_3)_3(\text{dppz-CN})]$ and $[\text{Eu}(\text{NO}_3)_3(\text{H}_2\text{O})_2(\text{dppz-CN})]$ complexes. All distances are given in Å.

	$[\text{Eu}(\text{NO}_3)_3(\text{H}_2\text{O})_2(\text{dppz-CN})]$		$[\text{Eu}(\text{NO}_3)_3(\text{dppz-CN})]$	
	Ground	Excited	Ground	Excited
Eu-N1	2.703	2.669	2.633	2.570
Eu-N5	2.657	2.631	2.649	2.585
Eu-O1	2.450	2.457	2.463	2.404
Eu-O2	2.469	2.481	2.483	2.453
Eu-O4	2.512	2.585	2.463	2.411
Eu-O6	2.588	2.487	2.479	2.451
Eu-O8	2.532	2.535	2.481	2.443
Eu-O9	2.539	2.534	2.468	2.428
Eu-O10 _(h2o)	2.620	2.592	-	-
Eu-O11 _(h2o)	2.598	2.604	-	-
C19-N8	1.163	1.167	1.163	1.167
C16-C19	1.428	1.418	1.428	1.417

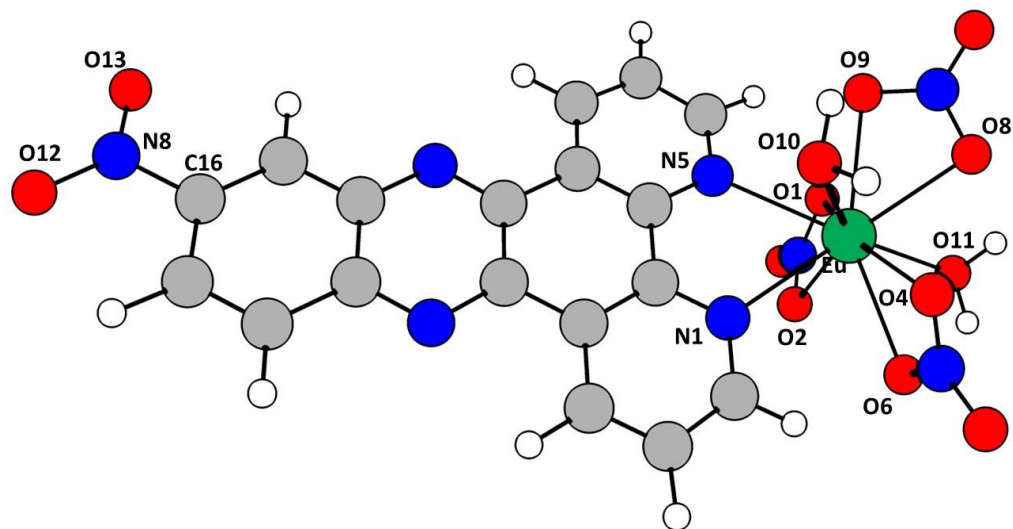
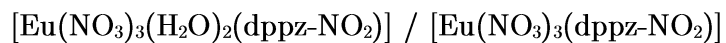


Table S1.3. Bond lengths for $[\text{Eu}(\text{NO}_3)_3(\text{dppz-NO}_2)]$ and $[\text{Eu}(\text{NO}_3)_3(\text{H}_2\text{O})_2(\text{dppz-NO}_2)]$ complexes. All distances are given in Å.

	$[\text{Eu}(\text{NO}_3)_3(\text{H}_2\text{O})_2(\text{dppz-NO}_2)]$		$[\text{Eu}(\text{NO}_3)_3(\text{dppz-NO}_2)]$	
	Ground	Excited	Ground	Excited
Eu-N1	2.706	2.666	2.609	2.569
Eu-N5	2.660	2.633	2.618	2.582
Eu-O1	2.450	2.458	2.419	2.394
Eu-O2	2.469	2.483	2.446	2.451
Eu-O4	2.511	2.492	2.421	2.408
Eu-O6	2.586	2.581	2.441	2.448
Eu-O8	2.531	2.537	2.442	2.441
Eu-O9	2.539	2.529	2.428	2.428
N8-O12 _(NO2)	1.235	1.245	1.234	1.244
N8-O13 _(NO2)	1.233	1.248	1.232	1.248
C16-N8	1.484	1.446	1.486	1.444
Eu-O10 _(h2o)	2.620	2.588	-	-
Eu-O11 _(h2o)	2.597	2.606	-	-

2. TD-DFT Calculations

dppz

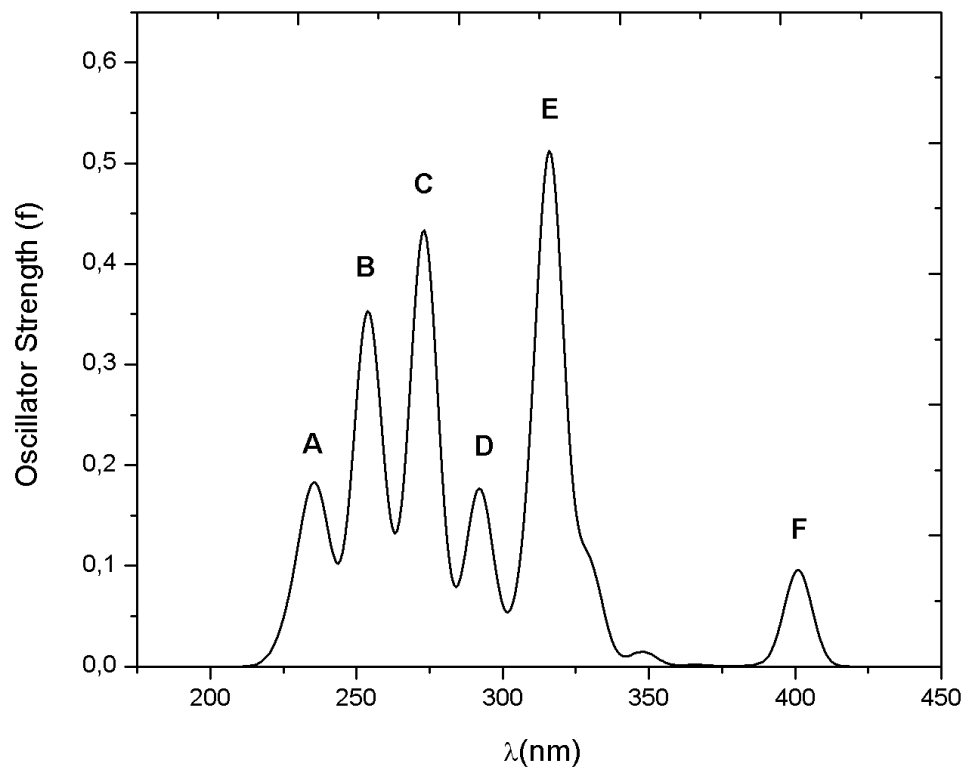
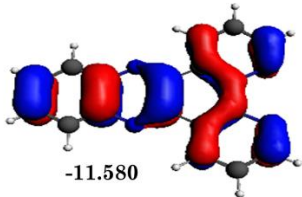
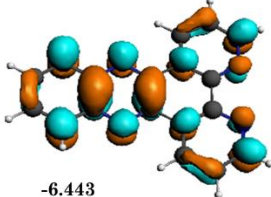
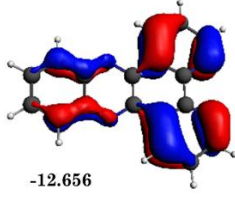
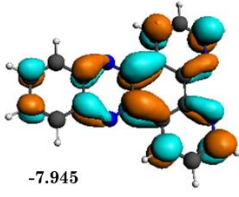
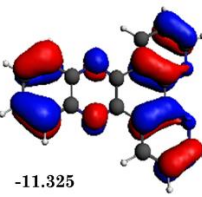
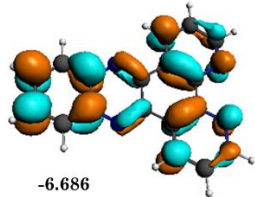
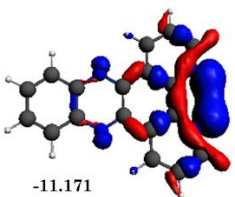
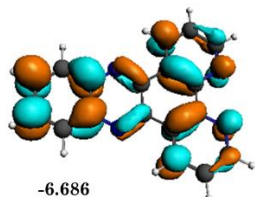
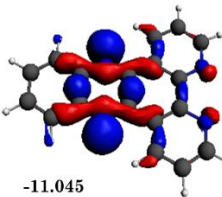
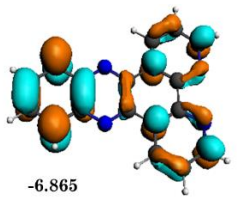
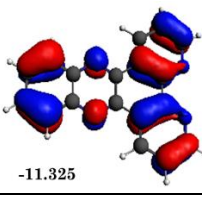
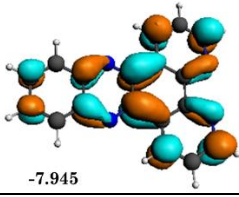
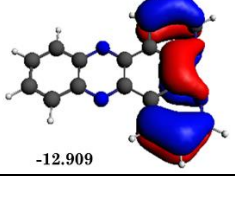
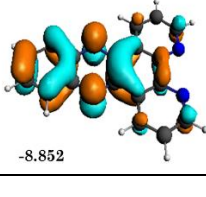
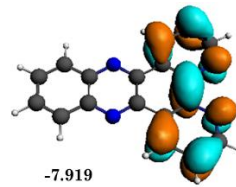
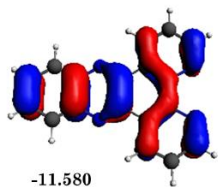


Table S2.1. Most relevant electronic transitions for dppz ligand.

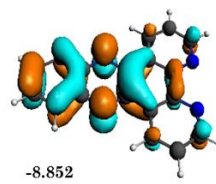
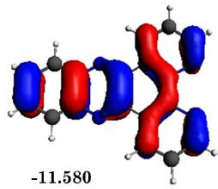
Band	$\lambda(\text{nm})$	E(eV)	f	%	Origin	Assignment
A	233.6	5.31	0.103	66.5	HOMO-4→LUMO+5	$\pi \rightarrow \pi^*$
B	253.7	4.89	0.333	42	HOMO-7→LUMO+1	$\pi \rightarrow \pi^*$
				35.5	HOMO-3→LUMO+4	$\pi \rightarrow \pi^*$
C	271.7	4.56	8.1E-08	91.6	HOMO-2→LUMO+4	$n \rightarrow \pi^*$
D	294.6	4.21	5.3E-05	93.3	HOMO-1→LUMO+3	$n \rightarrow \pi^*$
				43.4	HOMO-3→LUMO+1	$\pi \rightarrow \pi^*$
				18.2	HOMO-8→LUMO	$\pi \rightarrow \pi^*$
E	316.1	3.92	0.493	16.9	HOMO-4→LUMO+2	$\pi \rightarrow \pi^*$
				73.2	HOMO-4→LUMO	$\pi \rightarrow \pi^*$
F	400.9	3.09	0.095	73.2	HOMO-4→LUMO	$\pi \rightarrow \pi^*$

Table S2.2. Molecular Orbitals involved in the electronic transitions for dppz ligand. The energy of each molecular orbital is given in eV.

Band	Origin	
A	 -11.580	 -6.443
	 -12.656	 -7.945
B	 -11.325	 -6.686
	 -11.171	 -6.686
C	 -11.045	 -6.865
	 -11.325	 -7.945
D	 -12.909	 -8.852



F



dppz - Dichloromethane

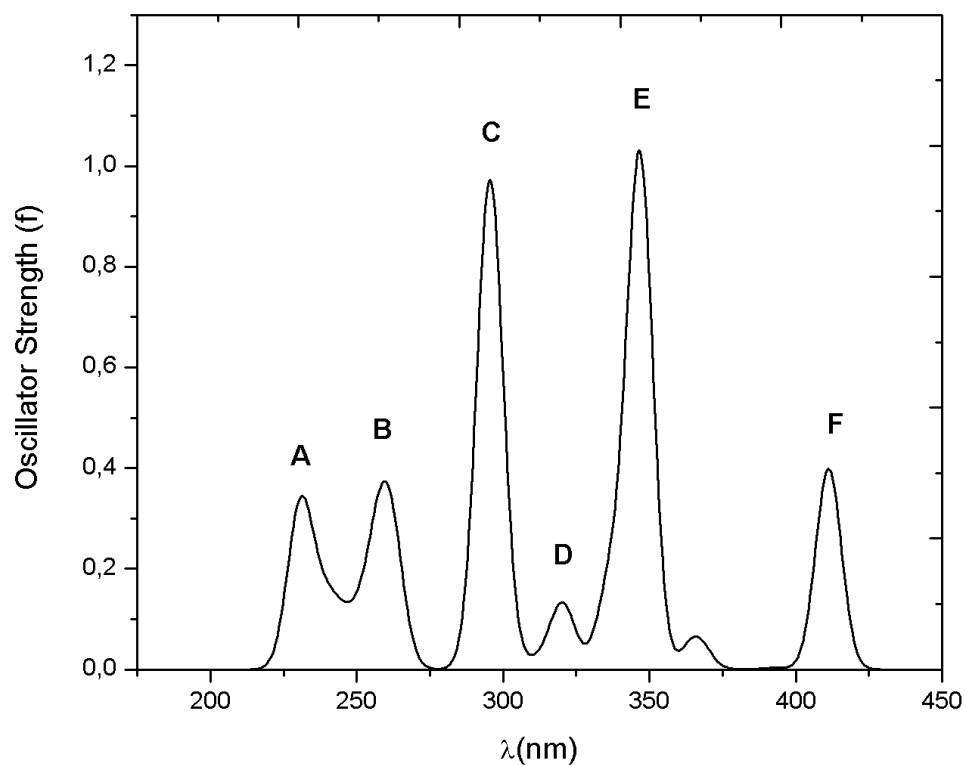
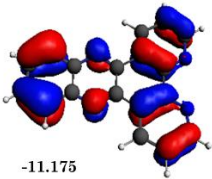
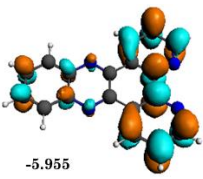
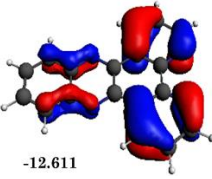
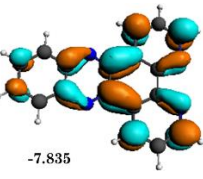
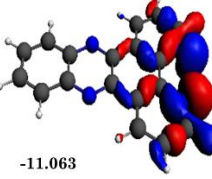
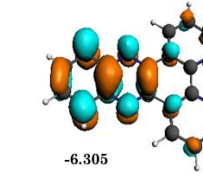
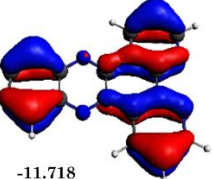
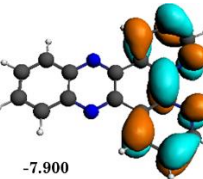
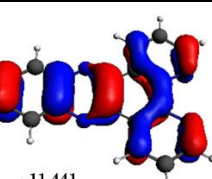
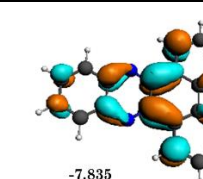
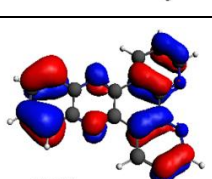
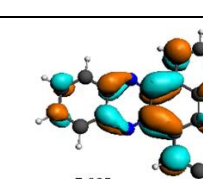
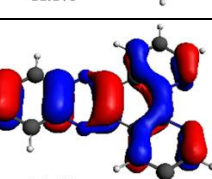
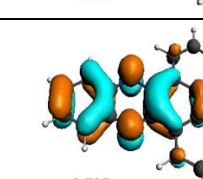


Table S2.3. Most important electronic transitions for dppz ligand with dichloromethane.

Band	$\lambda(\text{nm})$	$E(\text{eV})$	f	%	Origin	Assignment
A	231.4	5.35	0.364	34.7	HOMO-2→LUMO+6	$\pi \rightarrow \pi^*$
				15.3	HOMO-7→LUMO+2	$\pi \rightarrow \pi^*$
B	259.6	4.76	0.379	95.4	HOMO-1→LUMO+5	$n \rightarrow \pi^*$
C	295.7	4.19	0.896	59.2	HOMO-5→LUMO+1	$\pi \rightarrow \pi^*$
D	320.2	3.87	0.132	81.5	HOMO-3→LUMO+2	$\pi \rightarrow \pi^*$
E	346.7	3.58	1.017	81.7	HOMO-2→LUMO+2	$\pi \rightarrow \pi^*$
F	411.2	3.02	0.398	87.5	HOMO-3→LUMO	$\pi \rightarrow \pi^*$

Table S2.4. Molecular Orbitals involved in the electronic transitions for dppz ligand with dichloromethane. The energy of each molecular orbital is given in eV.

Band	Origin	
A	 -11.175	 -5.955
	 -12.611	 -7.835
B	 -11.063	 -6.305
	 -11.718	 -7.900
D	 -11.441	 -7.835
	 -11.175	 -7.835
F	 -11.441	 -8.707

dppz- CN

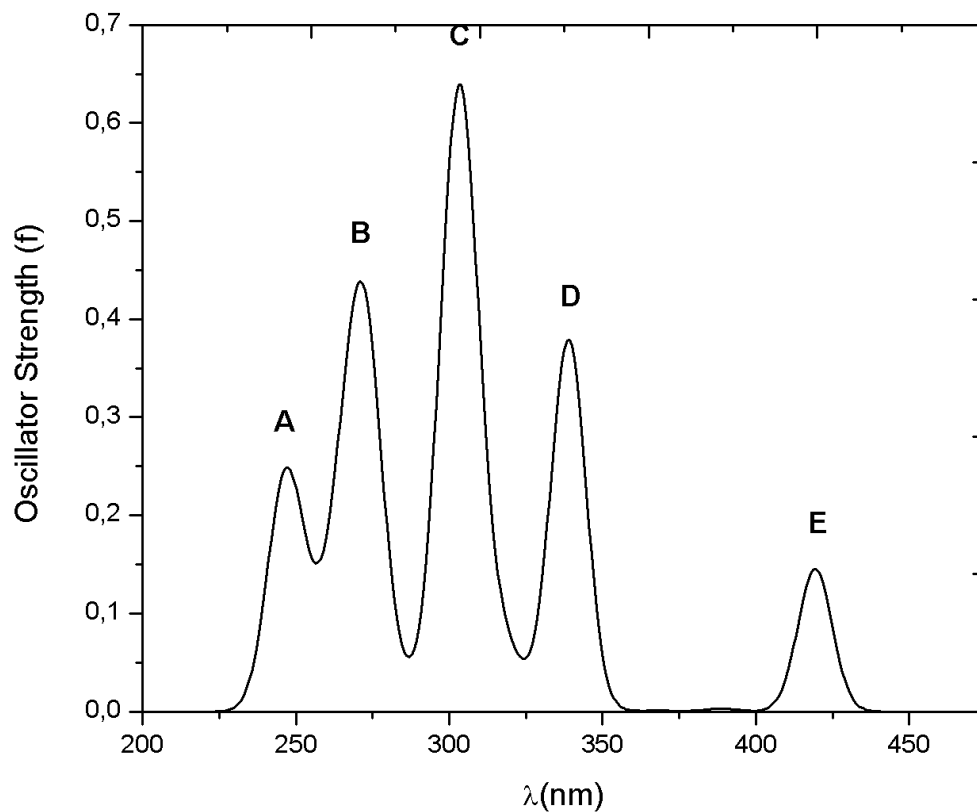
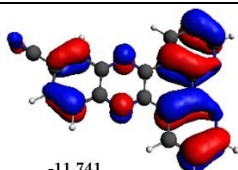
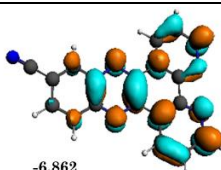
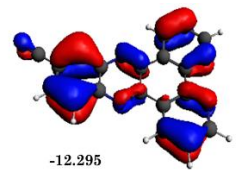
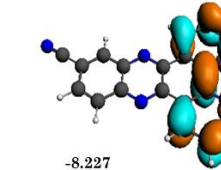
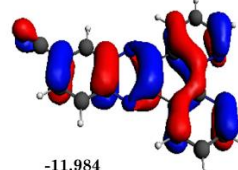
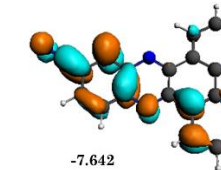
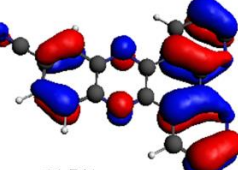
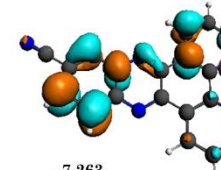
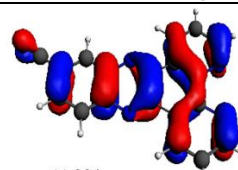
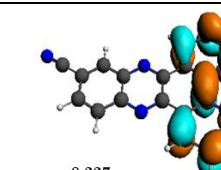
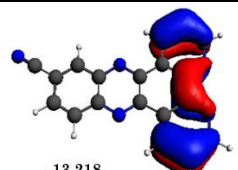
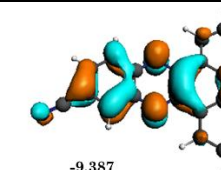
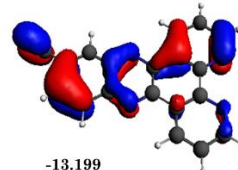
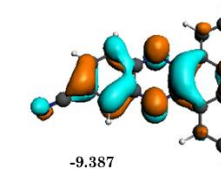

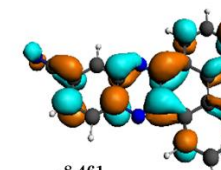


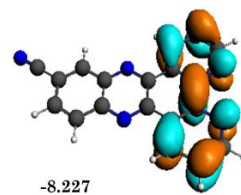
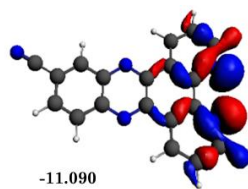
Table S2.5. Most important electronic transitions for dppz - CN ligand.

Band	λ (nm)	E(eV)	f	%	Origin	Assignment
A	249.3	4.97	0.059	46.0	HOMO-3→LUMO+5	$\pi \rightarrow \pi^*$
				25.3	HOMO-5→LUMO+2	$\pi \rightarrow \pi^*$
B	272.4	4.55	0.256	16.8	HOMO-4→LUMO+3	$\pi \rightarrow \pi^*$
				13.4	HOMO-3→LUMO+4	$\pi \rightarrow \pi^*$
				33.7	HOMO-4→LUMO+2	$\pi \rightarrow \pi^*$
C	304.2	4.08	0.317	20.7	HOMO-9→LUMO	$\pi \rightarrow \pi^*$
				10.8	HOMO-8→LUMO	$\pi \rightarrow \pi^*$
D	339.2	3.66	0.355	52	HOMO-3→LUMO+1	$\pi \rightarrow \pi^*$
E	419.6	2.96	0.12E-03	62.7	HOMO→LUMO+2	$n \rightarrow \pi^*$

Table S2.6. Molecular Orbitals involved in the electronic transitions for dppz -CN ligand. The energy of each molecular orbital is given in eV.

Band	Origin	
A	 -11.741	 -6.862
	 -12.295	 -8.227
B	 -11.984	 -7.642
	 -11.741	 -7.263
	 -11.984	 -8.227
	 -13.218	 -9.387
C	 -13.199	 -9.387
	 -11.741	 -8.461
D		

E



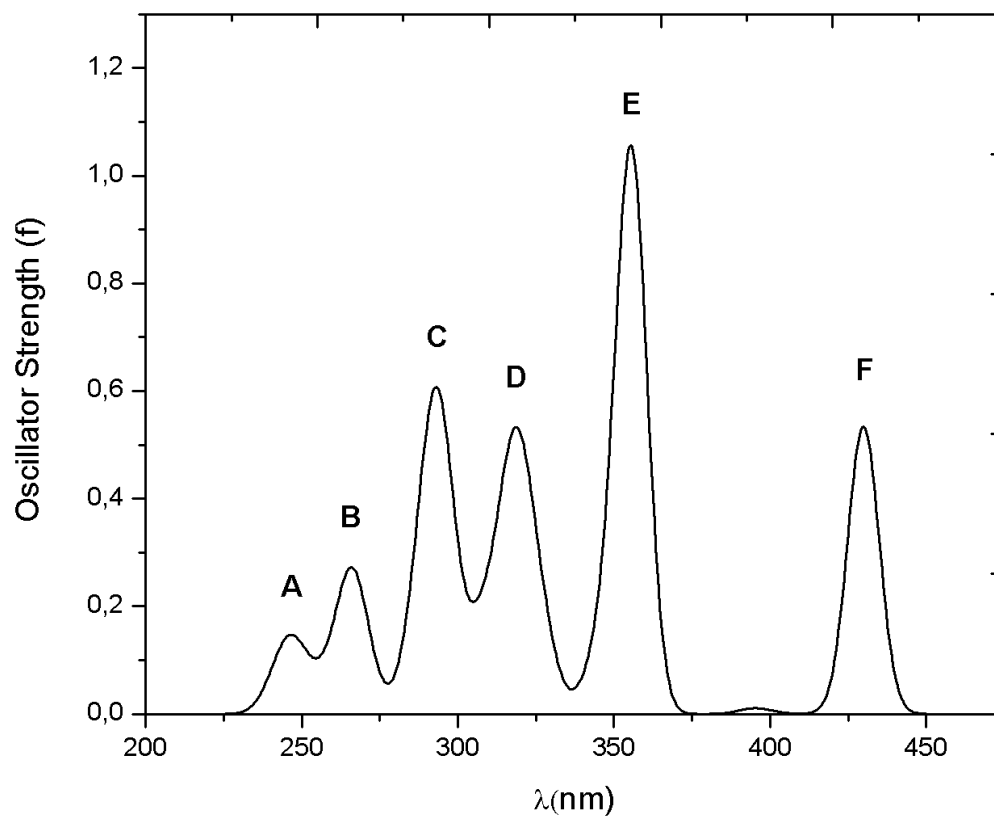
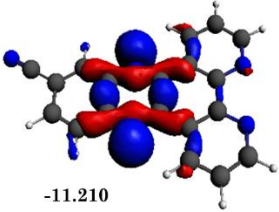
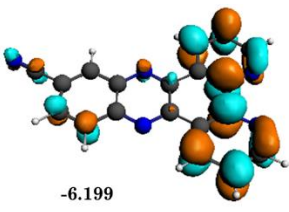
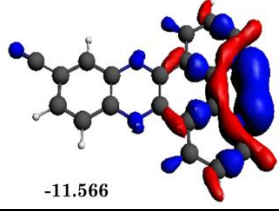
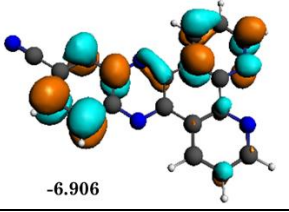
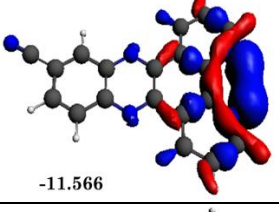
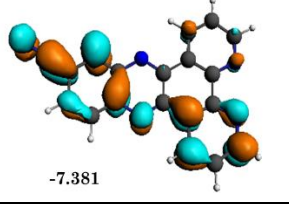
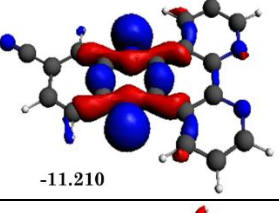
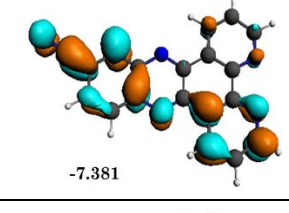
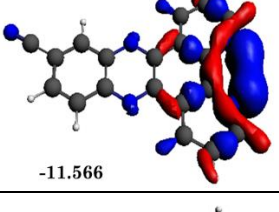
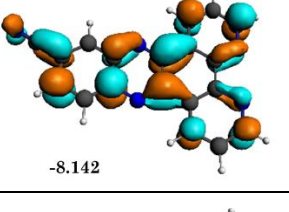
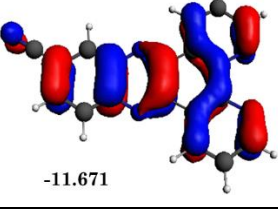
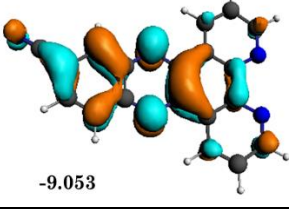


Table S2.7. Most important electronic transitions for dppz - CN ligand with dichloromethane.

Band	λ (nm)	E(eV)	f	%	Origin	Assignment
A	246.9	5.02	0.03	80.3	HOMO-1→LUMO+6	$n \rightarrow \pi^*$
B	267.4	4.64	0.1E-03	87.0	HOMO-3→LUMO+4	$n \rightarrow \pi^*$
C	294	4.22	0.6E-03	96.9	HOMO-3→LUMO+3	$n \rightarrow \pi^*$
D	318.2	3.89	0.2E-03	71.4	HOMO-1→LUMO+3	$n \rightarrow \pi^*$
E	358.9	3.45	2.6E-05	95.3	HOMO-3→LUMO+1	$n \rightarrow \pi^*$
F	429.9	2.88	0.534	91.2	HOMO-4→LUMO	$\pi \rightarrow \pi^*$

Table S2.8. Molecular Orbitals involved in the electronic transitions for dppz-CN ligand with dichloromethane. The energy of each molecular orbital is given in eV.

Band	Origin	
A	 -11.210	 -6.199
B	 -11.566	 -6.906
C	 -11.566	 -7.381
D	 -11.210	 -7.381
E	 -11.566	 -8.142
F	 -11.671	 -9.053

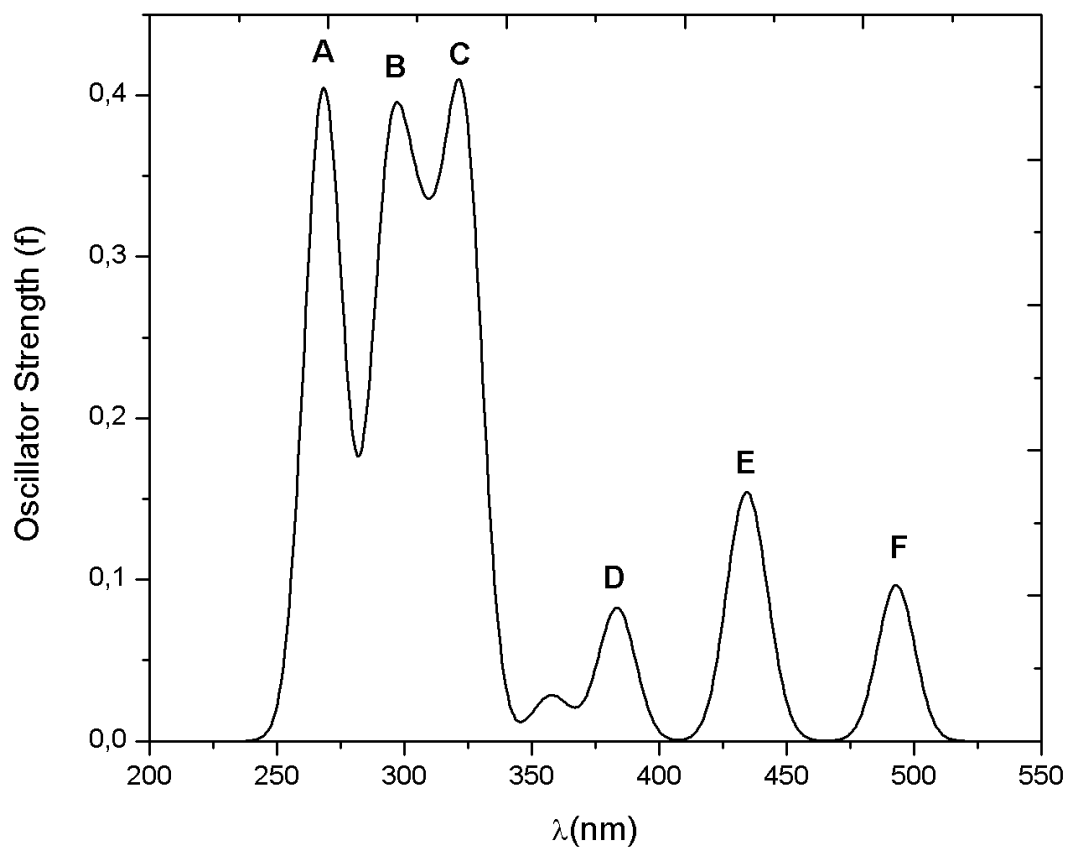
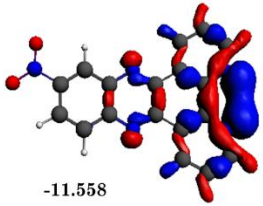
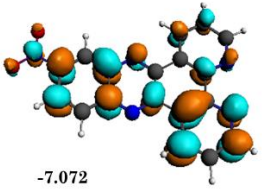
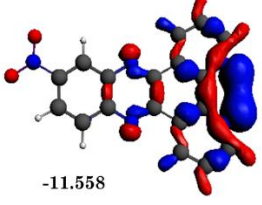
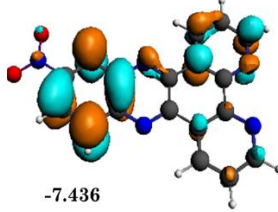
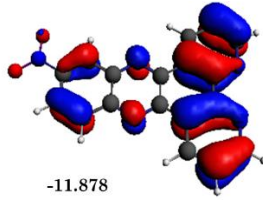
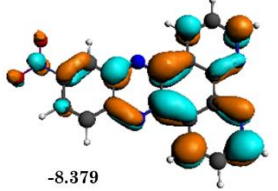
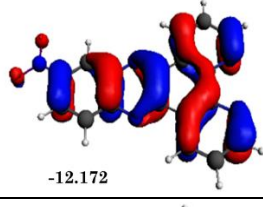
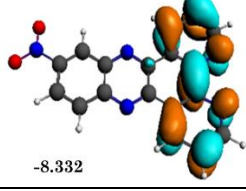
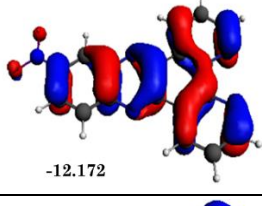
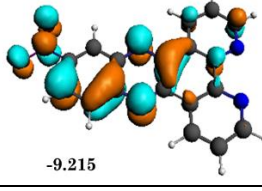
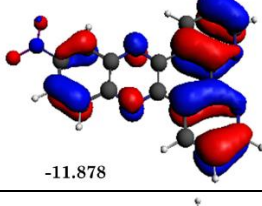
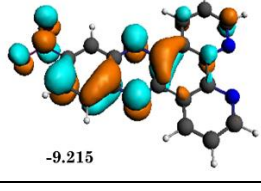
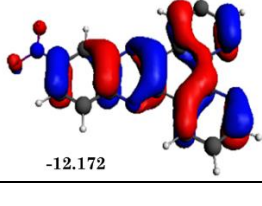
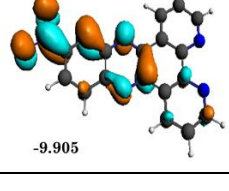


Table S2.9. Most important electronic transitions for dppz - NO₂ ligand.

Band	$\lambda(\text{nm})$	$E(\text{eV})$	f	%	Origin	Assignment
A	271.9	4.56	0.1E-03	88.9	HOMO-1→LUMO+5	$n \rightarrow \pi^*$
B	299.8	4.14	4.6E-06	81.3	HOMO-1→LUMO+4	$n \rightarrow \pi^*$
C	322.7	3.84	0.316	44	HOMO-3→LUMO+2	$\pi \rightarrow \pi^*$
				25.4	HOMO-4→LUMO+3	$\pi \rightarrow \pi^*$
D	383.5	3.23	0.082	74.3	HOMO-4→LUMO+1	$\pi \rightarrow \pi^*$
E	432.3	2.87	0.115	74	HOMO-3→LUMO+1	$\pi \rightarrow \pi^*$
F	492.9	2.52	0.091	79.4	HOMO-4→LUMO	$\pi \rightarrow \pi^*$

Table S2.10. Molecular Orbitals involved in the electronic transitions for dppz- NO₂ ligand. The energy of each molecular orbital is given in eV.

Band	Origin	
A	 -11.558	 -7.072
B	 -11.558	 -7.436
C	 -11.878	 -8.379
	 -12.172	 -8.332
D	 -12.172	 -9.215
E	 -11.878	 -9.215
F	 -12.172	 -9.905

dppz- NO₂ - Dichloromethane

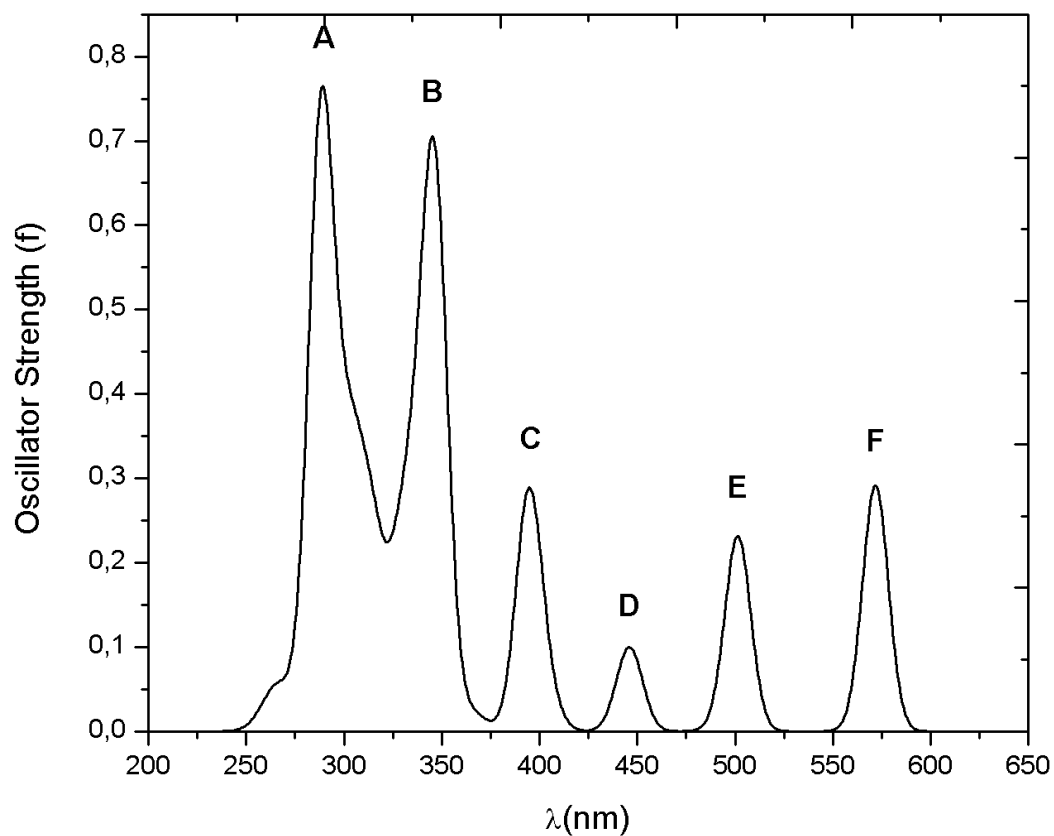
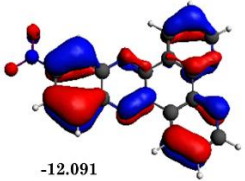
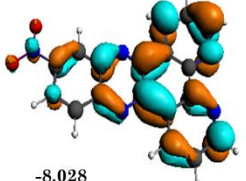
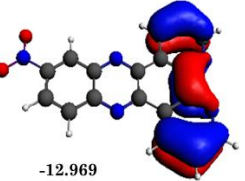
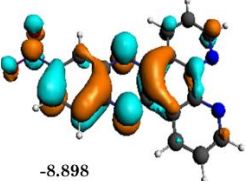
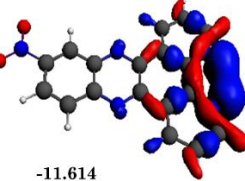
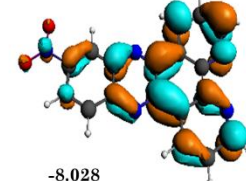
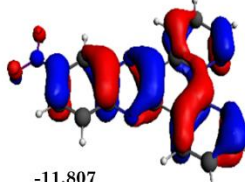
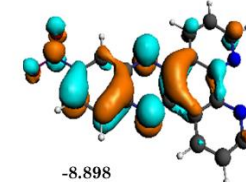
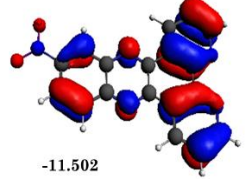
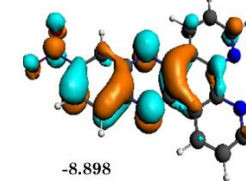
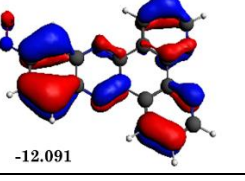
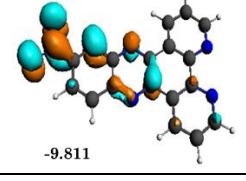
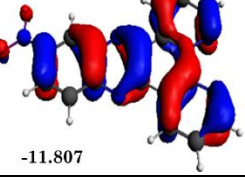
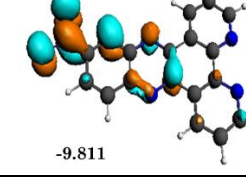


Table S2.11. Most important electronic transitions for dppz - NO₂ ligand with dichloromethane.

Band	λ (nm)	E(eV)	f	%	Origin	Assignment
A	289.9	4.28	0.02	30.3	HOMO-5→LUMO+3	$\pi \rightarrow \pi^*$
				22.7	HOMO-8→LUMO+1	$n \rightarrow \pi^*$
B	341.9	3.63	7.9E-05	89	HOMO-3→LUMO+3	$\pi \rightarrow \pi^*$
C	394.6	3.14	0.279	82.3	HOMO-4→LUMO+1	$\pi \rightarrow \pi^*$
D	445.9	2.78	0.099	92.4	HOMO-2→LUMO+1	$\pi \rightarrow \pi^*$
E	501.4	2.47	0.231	90.9	HOMO-5→LUMO	$\pi \rightarrow \pi^*$
F	571.8	2.17	0.292	93.3	HOMO-4→LUMO	$\pi \rightarrow \pi^*$

Table S2.12. Molecular Orbitals involved in the electronic transitions for dppz - NO₂ with dichloromethane. The energy of each molecular orbital is given in eV.

Band	Origin	
A	 -12.091	 -8.028
	 -12.969	 -8.898
B	 -11.614	 -8.028
	 -11.807	 -8.898
C	 -11.502	 -8.898
	 -12.091	 -9.811
D	 -11.807	 -9.811

3. Spin orbit energies for the low-lying states in the europium fragment

Table S3. SO-CASPT2 energies for the Eu^{III} fragments. All the energies are given in cm^{-1} .

State	$\text{Eu}(\text{NO}_3)_3$	$\text{Eu}(\text{NO}_3)_3(\text{H}_2\text{O})_2$
J = 0	0.0	0.0
J = 1	120.6	282.2
	590.3	459.5
	718.6	494.2
J = 2	1214.2	1011.8
	1272.7	1033.2
	1372.3	1084.9
	1400.8	1254.0
	1497.0	1346.1
J = 3	2080.6	2024.7
	2207.2	2055.2
	2284.4	2065.6
	2310.1	2102.4
	2376.9	2118.9
	2395.1	2139.6
	2434.1	2255.9
J = 4	3136.4	2808.6
	3158.7	3076.9
	3267.9	3120.5
	3425.5	3152.6
	3435.3	3220.3
	3490.8	3228.4
	3518.1	3312.1
	3540.9	3340.3
	3554.2	3387.1
	4018.6	4048.7
	4043.0	4071.1
	4332.2	4120.2
	4344.5	4160.6
	4547.4	4258.8

J = 5	4609.2	4306.9
	4639.4	4370.8
	4672.9	4390.2
	4686.0	4408.8
	4733.4	4410.5
	4746.4	4444.6
J = 6	4773.6	5022.6
	4796.2	5028.9
	5332.9	5200.0
	5338.7	5218.7
	5534.9	5263.2
	5550.0	5277.4
	5678.3	5307.7
	5709.7	5319.2
	5775.8	5336.9
	5826.1	5395.3
	5845.2	5398.4
	5935.2	5467.0
	5936.7	5468.0

4. Experimental Section

General methods and materials

All chemicals were reagent-grade, purchased from Aldrich and used as received unless otherwise specified. NMR spectra were recorded using a Bruker AVANCE 400 spectrometer at 25°C. The samples were dissolved in deuterated dichloromethane, using tetramethylsilane as an internal reference. Aldrich spectroscopic grade or HPLC grade solvents were used for all spectroscopic measurements. Infrared spectra were recorded on a Perkin Elmer FTIR Spectrum Two and an UATR Two accessory was used in measurements of the sample in the solid state. Fluorescence measurements were acquired at room temperature and with solid samples on a spectrometer FLUOROLOG 3 ISA/Jobin-Yvon, equipped with a Hamamatsu R928P photomultiplier and a 450 W xenon lamp (ozone free). Elemental analysis was performed on a Perkin-Elmer model Perkin-Elmer 2400 Series-II elemental analyzer instrument. Mass spectra samples were analyzed with a hybrid LTQ FT (ICR 7T) (ThermoFisher, Bremen, Germany) mass spectrometer. Samples were introduced via a microelectrospray source at a flow rate of 3 mL min⁻¹. For X-ray powder diffraction measurements, the samples were pulverized and measured at room temperature in a X-ray diffractometer SHIMADZU, model XRD-6000, with Cu-K α radiation (λ =1.5418 Å), diffraction angle (2θ) varying from 5 to 90° (increment of 0.01°, voltage of 40 kV and current of 30 mA).

Crystal structures cannot be obtained due to poor solubility of the samples. However, elemental analysis, Fourier Transform Infrared (FT-IR) spectroscopy, ultraviolet-visible, absorption (UV-vis) spectroscopy, photoluminescence (PL) studies, mass spectrometry and X-ray studies (powder XRD) confirm the identity of the complexes

studied here. FT-IR study shows the characteristic bands of the ligand and its complexes. The IR spectrum of the dppz-CN ligand shows bands at 3060, 2227 and 1584 cm^{-1} , which may be assigned to $\nu(\text{CH aromatic})$; $\nu(\text{C}\equiv\text{N})$; $\nu(\text{C}=\text{N})$, whereas in dppz-NO₂ the bands is located at 3061 $\nu(\text{CH aromatic})$, 1522 $\nu(\text{NO}_2)$, 1343 $\nu(\text{NO}_2)$. In the Europium complexes, these bands are shifted, indicating that there are a coordination between the ligand and the lanthanide ion. The absorption bands assigned to the coordinated nitrates were observed for both complexes as a group bands at about 1495 (s, NO₃⁻), 1299 (s, NO₃⁻), 1081 (s, NO₃⁻) for dppz-CN and 1491(s, NO₃⁻), 1287 (s, NO₃⁻), 1026 (s, NO₃⁻) for dppz-NO₂, respectively. Differences between the strongest absorption bands of nitrate group are 196 cm^{-1} and 204 cm^{-1} , this separation of the two highest frequencies has been extensively studied in nitrate complexes.^{1,2} In general larger separations are an indicator of that coordinated nitrate groups in the complexes are bidentate.

Figures S1 and S2 show the experimental X-ray diffraction powders for Eu^{III} complexes and dppz-R ligands obtained in this work. The patterns were analyzed and compared with the crystallographic data JCPDS (Joint Committee on Powder Diffraction Standards) of the International Centre for Diffraction Data, available in the software Crystallographica Search-Match. Typical patterns for free ligands and Eu^{III} complexes are shown by the profiles, which clearly indicates that different structures and coordination environments are adopted. Thus, dppz-R ligands could form stable complexes with Eu^{III} ion.

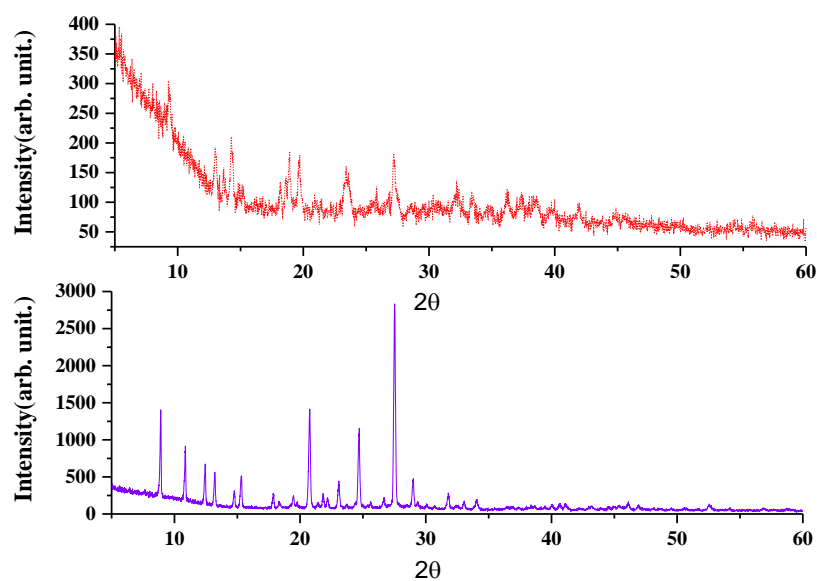


Figure S1. Top: experimental X-ray diffraction diagrams of the powders obtained with $[\text{Eu}(\text{NO}_3)_3(\text{dppz-CN})]$ Bottom: experimental X-ray diffraction powders for dppz-CN.

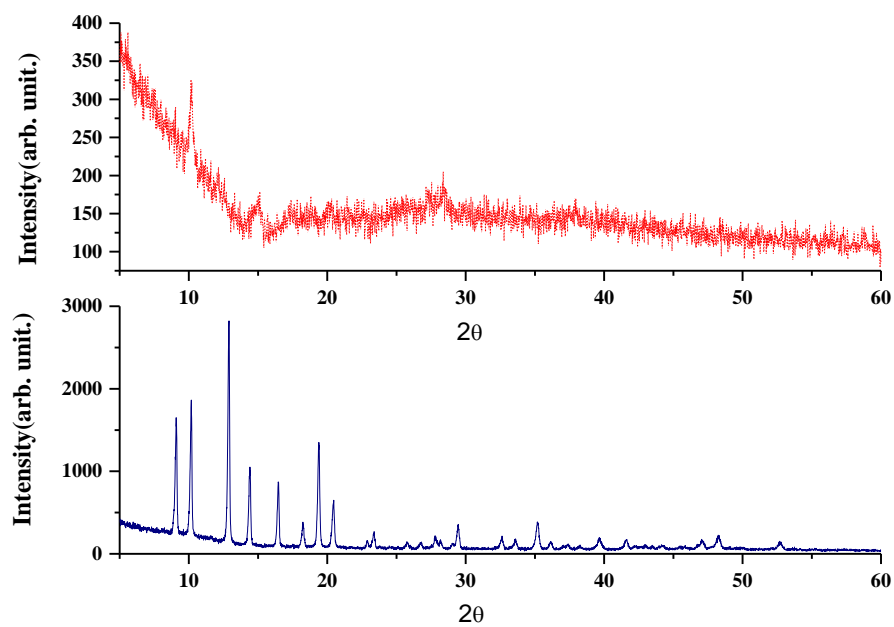


Figure S2. Top: experimental X-ray diffraction diagrams of the powders obtained with $[\text{Eu}(\text{NO}_3)_3(\text{dppz-NO}_2)]$ Bottom: experimental X-ray diffraction powders for dppz- NO_2 .

Synthesis and characterization

The ligands and complexes prepared in this work, were synthesized following a generalized synthetic procedure³ which is described below. The ligands were characterized by elemental analysis, infrared (FT-IR) spectroscopy, NMR spectra, and X-ray studies (powder XRD). Additionally to this techniques (except NMR spectra), the synthesized europium complexes were characterized by ultraviolet-visible, absorption (UV-vis) spectroscopy, photoluminescence (PL) studies, mass spectrometry.

a. Synthesis of 11-cyanodipyrido[2,3-a:2',3'-c]phenazine (dppz-CN)

4.80 mmol of 1,10-phenanthroline-5,6-dione and 4.80 mmol of 3,4-diaminobenzonitrile were dissolved in 80 mL of methanol and the mixture was refluxed for 5 h. The mixture was allowed to cool and the resultant precipitate filtered and washed with MeOH and diethyl ether to give a light red solid that was dried in vacuum. Anal. Calc. for C₁₉H₉N₅: C, 74.27; H, 2.94; N, 22.79. Found: C, 74.26; H, 2.94; N, 22.84%. IR (cm⁻¹): 3060 m(CH aromatic); 2227 m(C≡N); 1584 m(C=N). ¹H NMR (CDCl₃, 400 MHz, δ ppm): 7.68–7.73 (m, 2H, Hc and Hc'); 7.95 (dd, 1H, Ha'); 8.29 (d, 1H, He); 8.57 (d, 1H, Ha); 9.22–9.25 (m, 2H, Hd and Hd'); 9.35–9.42 (m, 2H, Hb and Hb').

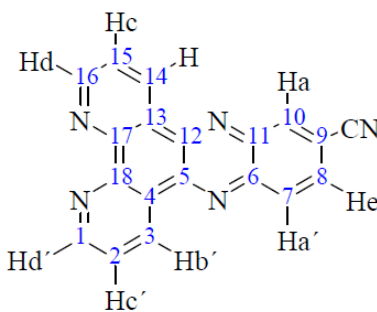


Figure S3. Proton and carbon numbering for the NMR signals of the dppz-CN ligand.

b. Synthesis of 11-nitrodipyrido[2,3-a:20,30-c]phenazine (dppz-NO₂)

1.43 mmol of 1,10-phenanthroline-5,6-dione and 6.53 mmol of 1,2-diamino-4-nitrobenzene were dissolved in 40 mL of dry ethanol and the mixture refluxed for 2h. After cooling, the yellow precipitate was collected by filtration, washed with cold ethanol, and vacuum-dried. Anal. Calc. for C₁₈H₉N₅O₂: C, 66.05; H, 2.77; N, 21.39. Found: C, 66.10; H, 2.80; N, 21.74%. IR(cm⁻¹): 3061 m(CH aromatic), 1522 v(NO₂) , 1343 v(NO₂), ¹H NMR (CDCl₃, 400 MHz, δ ppm): 9.69–9.67 (m, 2H, Hc and Hc'), 9.39- 9.38 (d ,2H,Ha and Ha'),7.88-7.91(m, 2H, Hb and Hb') 8.68 (d, 1H, He), 9.27- 8.52(m, 2H, Hd and Hd').

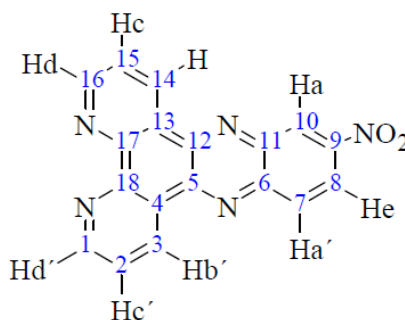
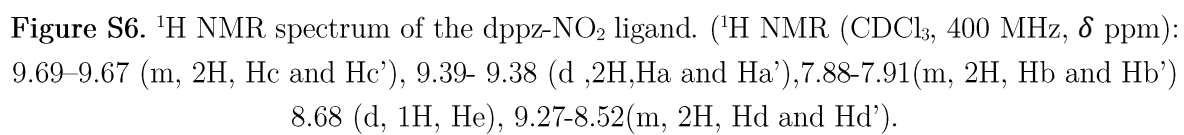
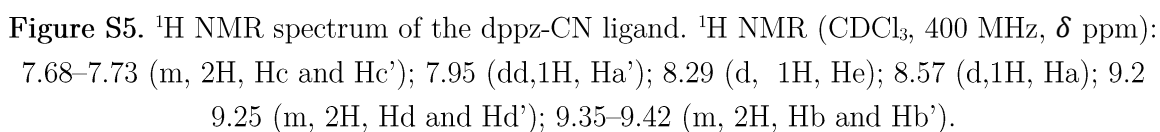


Figure S4. Proton and carbon numbering for the NMR signals of the dppz-NO₂ ligand

c. Characterization of europium [Eu(NO₃)₃ (dppz-R)] complexes

[Eu(NO₃)₃(dppz-CN)] (**2**). Yield (78%).Anal. calc. for C₃₈H₁₈EuN₁₃O₉. C, 47.91; H, 1.90; N, 19.11. Found: C, 47.95; H, 2.01; N, 19.14. ESI-MS Calcd (found): m/z 954.22 IR (cm⁻¹): 3051 m (CH aromatic); 2273 m(C≡N); 1594 (C=N), 1495(s,NO₃⁻), 1299(s,NO₃⁻), 1081(s,NO₃⁻).

[Eu(NO₃)₃(dppz-NO₂)] (**3**). Yield:(75%).Anal. calc. for C₃₆H₁₈EuN₁₃O₁₃. C, 43.56; H, 1.82; N, 18.34. Found: C, 43.78; H, 1.90 ; N, 18.75. ESI-MS Calcd (found): m/z 993.45 IR (cm⁻¹): 3086 m (CH aromatic); 2284 m(C≡N); 1578 (C=N), 1491(s,NO₃⁻), 1287(s,NO₃⁻), 1026(s,NO₃⁻).



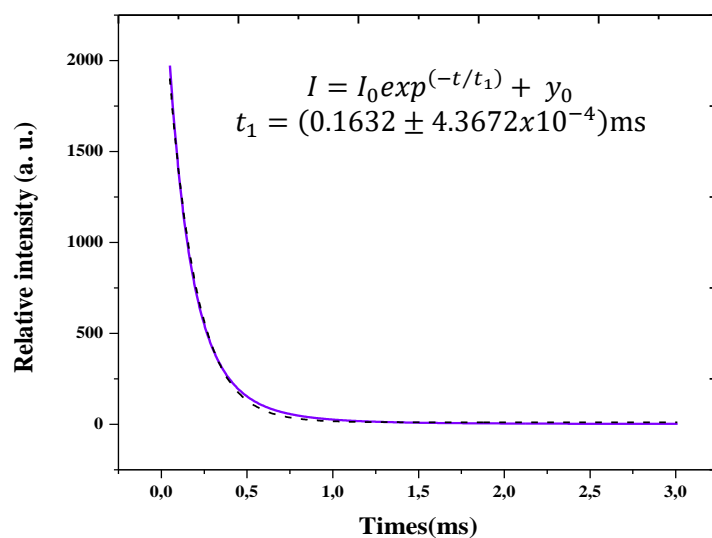


Figure S7. Decaying of the luminescence of the emitting 5D_0 Eu^{III} state of the $[\text{Eu}(\text{NO}_3)_3(\text{dppz-CN})]$. Violet line: data; dashed line: fitting. A single-exponential decaying function fitting ($R^2 = 0.997$) yielded a value of $\tau = (0.1632 \pm 4.3672 \times 10^{-4})$ ms.

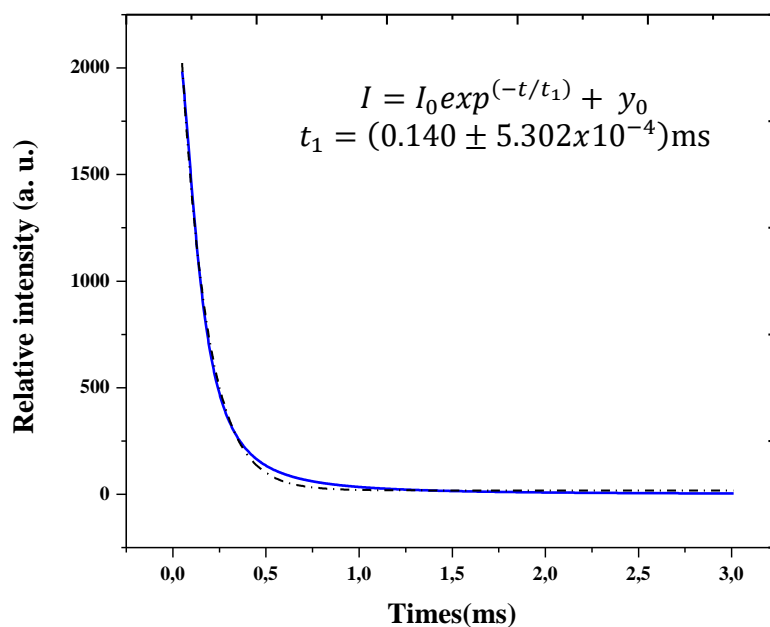


Figure S8. Decaying of the luminescence of the emitting 5D_0 Eu^{III} state of the $[\text{Eu}(\text{NO}_3)_3(\text{dppz-NO}_2)]$. Blue line: data; dashed line: fitting. A single-exponential decaying function fitting ($R^2 = 0.996$) yielded a value of $\tau = (0.140 \pm 5.302 \times 10^{-4})$ ms.



Figure S9. Film of complex $[\text{Eu}(\text{NO}_3)_3 (\text{dppz-NO}_2)]$ deposited in a round bottom flask, illuminated by a black light (ultraviolet light) lamp

References

- (1) Zhang, Y.; Qin, W.; Liu, W.; Tan, M.; Tang, N. Studies on Synthesis and Infrared and Fluorescence Spectra of New Europium and Terbium Complexes with an Amide-based Open-chain Crown Ether. *Spectrochim. Acta A Mol. Biomol. Spectrosc.* **2002**, *58*, 2153–2157.
- (2) Nakamoto, K. *Infrared and Raman Spectra of Inorganic and Coordination Compounds: Part A: Theory and Applications in Inorganic Chemistry.*; John Wiley & Sons: Marquette University, New Jersey, 2009; p. 432.
- (3) Zúñiga, C.; Crivelli, I.; Loeb, B. Synthesis, Characterization, Spectroscopic and Electrochemical Studies of Donor–acceptor ruthenium(II) Polypyridine Ligand Derivatives with Potential NLO Applications. *Polyhedron* **2015**, *85*, 511–518.